

Project Nighthawk NOAA 2018 Manoomin Airborne Hyperspectral Project

Final Report

by

Galileo Group, Inc.

January 25, 2019

Principal Authors:

John Merrill, MSc

Thorsten Mewes, PhD



Table of Contents

1. INTRODUCTION	4
2. EQUIPMENT	5
3. DATA COLLECTION	7
4. DATA PROCESSING AND QC	24
5. ANALYSIS	27
6. CONCLUSION	30
7. APPENDIX A	31
8. APPENDIX B	36

1. Introduction:

Wild Rice (Manoomin) plays an integral role in the ecosystems, culture, and economy of the Lake Superior region and it faces an existential threat from invasive species which compete for the same habitat and a variety of other factors. The goal of this mission was to collect, pre-process, and analyze airborne hyperspectral imagery around the periphery of Lake Superior for the purpose of delineating Wild Rice and other types of aquatic vegetation. Six Areas of Interest (AOI) were identified as pilot sites and selected as the target AOI for this project.

AOI/Pilot Sites

1. Crooked Lake, Sucker Lake, and the Ontonagon River (CSO)
2. Eastern Upper Peninsula (EUP)
3. Fond du Lac (FDL)
4. Kakagon Sloughs and Bad River (KSBR)
5. St. Louis River Estuary (SLRE)
6. Upper St. Louis River (USLR)

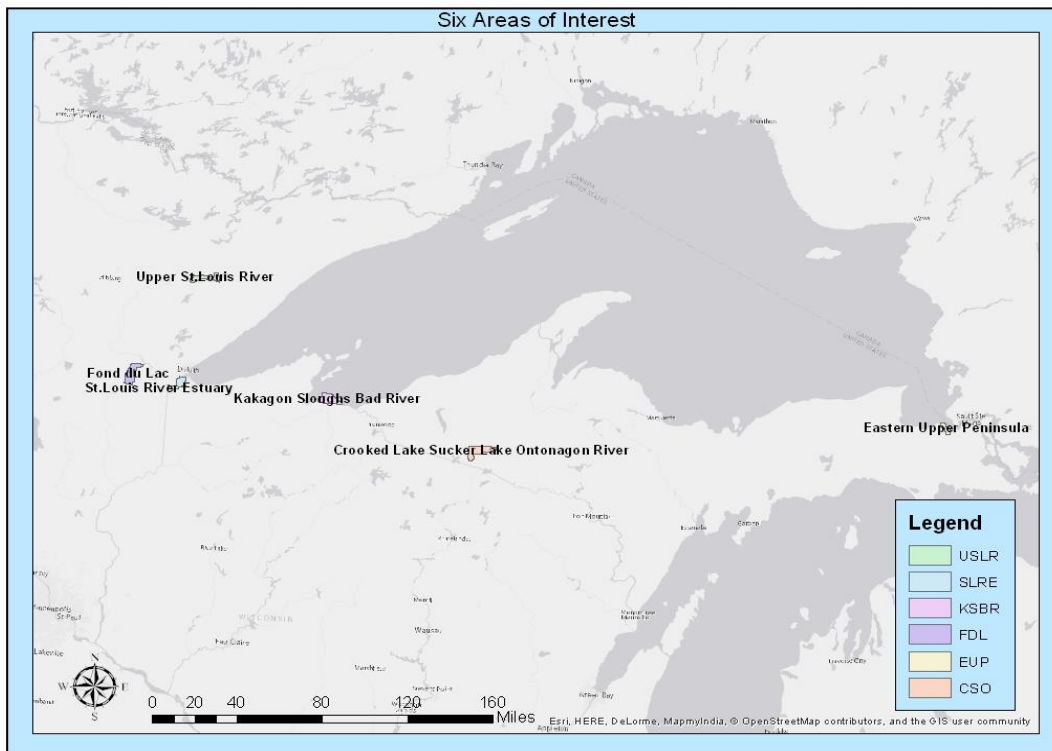


Figure 1: AOI Map

Airborne data collection commenced on 30 August and finished on 7 September. At the conclusion of airborne operations, extensive ground truthing operations were also conducted in order to located areas of Wild Rice and the other target species and to collect ground data that consisted of spectrometry, GPS points and geo-tagged imagery. This ground truthing data was used to train a supervised classification algorithm by providing known locations and spectral signatures of the target species. Analysis of the hyperspectral data was then performed on the airborne imagery and classified polygons were created for each of the 10 target classes (listed below).

Classes

1. Wild Rice (*Zizania palustris*) **Primary species of special concern**
2. Arrowhead (*Sagittaria latifolia*)
3. Burreed (*Sparganium eurycarpum*)
4. Cattail (*Typha angustifolia*, *Typha latifolia*, *Typha x glauca*)
5. Open Water
6. Other Emergent Aquatic Species
7. Phragmites (*Phragmites australis*)
8. Pickerelweed (*Pontederia cordata*)
9. Waterlily (*Nymphaea ordata*, *Nuphar variegata*)
10. Watershield (*Brassenia schreberi*)

2. Equipment

An AISA EAGLE II Visual through Near Infrared (VNIR) Hyperspectral Imaging Sensor System (400 – 1,000 nm spectral range) was utilized by Galileo Group Inc. (Galileo) for airborne collection operations. A total of 128 spectral bands for the VNIR (Visible Near Infrared) range were collected with a spectral resolution of around 5nm and a Ground Sampling Distance (GSD) of 1.0m. The FOV (Field of View) was 34 degrees. An Oxford Solutions Survey+ 2nd Generation GPS/IMU simultaneously collected navigation and attitude data. The sensor system was installed in a Cessna 172 Skyhawk which was used as the airborne imaging platform for the duration of the project.

AisaEAGLE

OPTICAL CHARACTERISTICS		TYPICAL SPECIFICATIONS			
Spectrograph	High efficiency transmissive imaging spectrograph. Throughput practically independent of polarization. Smile and keystone < 2 microns.				
Numerical aperture	F/2.4				
Spectral range	400-970 nm				
Spectral resolution	3.3 nm				
FODIS (optional)	Diffuse down welling irradiance collector and fiber optic cable (5 m standard) with SMA connector				
Calibration	Sensor provided with wavelength and radiometric calibration file.				
FORE OPTICS					
Fore optics options	OLE23	OLE18,5	OLE9		
FOV	29.9 degrees	37.7 degrees	Wide FOV lens More specifications upon request		
IFOV	0.029 degrees	0.037 degrees			
Swath width	0.53 x altitude	0.68 x altitude			
Ground resolution @ 1000 m altitude	0.52 m	0.68 m			
ELECTRICAL CHARACTERISTICS					
Detector	Progressive scan CCD detector				
Spectral binning options	1x	2x	4x	8x	
Number of spectral bands	488	244	122	60	
Spectral sampling/band	1.25 nm	2.3nm	4.6nm	9.2nm	
Frame rate, up to (frames/s)	30	59	100	160	
Spatial pixels	Up to 1024, of which 70 - 80 FODIS pixels (optional)				
Output	12 bits digital				
SNR	1250:1 (maximum theoretical) More detailed SNR data in various conditions available from SPECIM.				
Integration time	Adjustable, independent of image rate				
Shutter	Electromechanical shutter for dark background registration, user-controllable by software.				
Operating modes	Hyperspectral and multispectral The operator can create application specific band configurations, and quickly change from one mode or configuration to others in flight operation.				
Power consumption					
Complete system with rack PC	350 W				
Complete system with lightweight PC	220 W				
ENVIRONMENTAL CHARACTERISTICS					
Storage	- 20 ... +50 °C				
Operating	+ 5 ... +40 °C, non-condensing				

Figure 2: AISA Eagle II Datasheet

Ground truthing was conducted primarily onboard a canoe and along the shoreline where accessible. An ASD Fieldspec Pro VNIR (400-1000nm) was utilized to collect spectrometry of Wild Rice when found. A Trimble XRT Pro DGPS system and two handheld digital cameras with integrated GPS were used to collect GPS points and geo-tagged imagery of target species and landmarks of interest.



Figure 3: ASD Fieldspec Pro VNIR

3. Data collection

On 28 Aug 2018 the airborne hyperspectral imaging system, which consisted of an AISA Eagle II VNIR Hyperspectral Imaging Sensor, an OxTS Survey+ 2nd Generation GPS/IMU, and a flight computer, was installed by Galileo scientist Dr. Thorsten Mewes in a specially modified Cessna 172 aircraft. The sensor is annually calibrated using Galileo's integrating sphere and radiative lamps. Appendix B contains graphs of the sensor's radiometric calibration coefficient and radiance sensitivity. Below is a graph of the sensor's Signal to Noise Ratio (SNR).

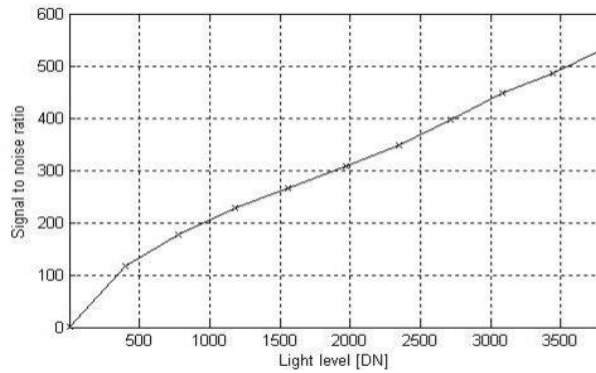


Figure 4: AISA Eagle II Signal to Noise Ratio

After completing the installation, Dr. Mewes then calculated a lever arm correction based on the installation geometry of the sensor system and the dual GPS antennas equipped on top of the aircraft. This information was then used to configure and calibrate the GPS/IMU using manufacturer software. A successful ground test of the entire system was then performed to ensure all systems were in good working order. Then, the pilot and sensor operator John Merrill transited to the Richard I. Bong Airport in Superior, WI. The aircraft and aircrew arrived safely in Superior, WI on 29 Aug 2018 and began data collection the next day.



Figure 5: Cessna 172 Skyhawk Aircraft



Figure 6: Bottom View of Aircraft Camera Port and Sensor Lens

Clear skies allowed aerial data acquisition to begin on 30 Aug 2018. Using manufacturer control and collection software, Mr. Merrill configured the sensor system into 128 spectral bands with a spectral resolution of approximately 4.6 nm. Integration time for all imagery was set to 12ms. Flight altitude for all six sites was set at 4500ft Above Ground Level (AGL) in order to produce 1m Ground Sampling Distance (GSD) for all pixels in the airborne hyperspectral imagery. Sensor frame rate was determined by aircraft speed which varied due to high winds aloft. The following table shows the frame rates used at each speed:

Aircraft Speed (Knots)	90	100	110
Sensor Frame Rate (frames per second)	50	56	62

Aerial data acquisition continued on September 1st, 3rd, 6th and wrapped up on the 7th. In total 136 flight lines were collected including four lines for the boresight calibration and 16 lines were collected twice due to the presence of clouds and shadows in the imagery. There were no problems with the sensor system or aircraft for the duration of collection operations. Once Mr. Merrill finished field processing the data and confirmed 100% coverage with no shadows or clouds and excellent spectral quality, then aerial data acquisition was wrapped up and the aircraft sent back to its home airport. Flight logs for all collection sorties are included at the end of this report as Appendix A. These logs contain all flight parameters and notes from the sensor operator.

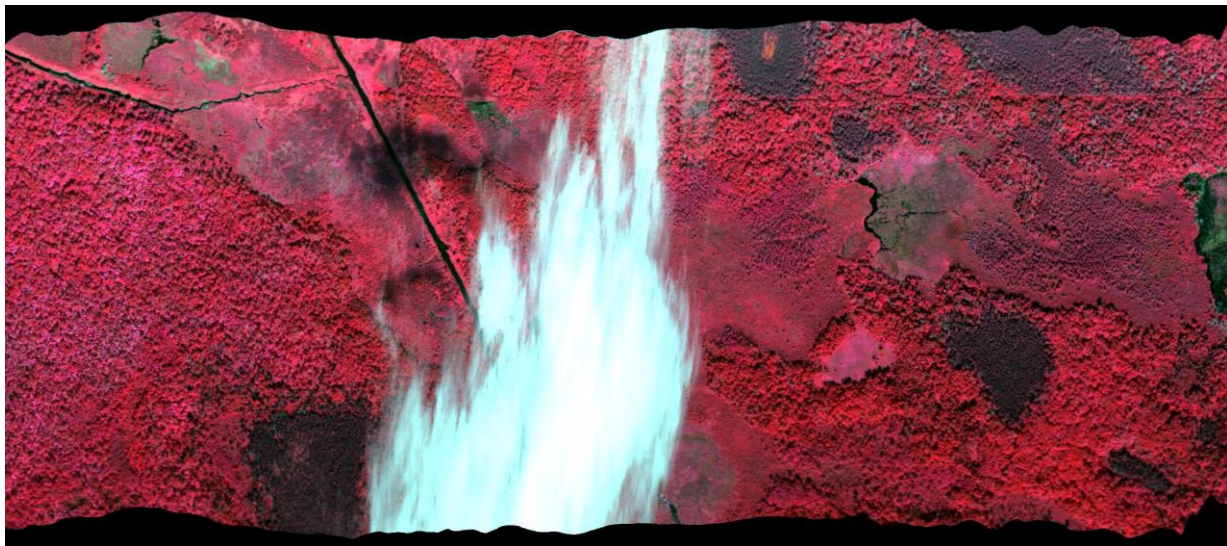


Figure 7: Clouds and shadows in flight line 0830-1246

Site 1: Fond du Lac

All 30 of the flight lines for the Fond du Lac site were collected on 30 August 2018, but the five northernmost flight lines contained scattered clouds and shadows, so these lines were re-collected on 3 September. Below are two mosaic images of the Fond du Lac site. On the left is a Color Infrared (CIR) mosaic with the site boundary as the green polygon. On the right is a Lookup Table (LUT) mosaic that shows the coverage of each individual flight lines as strips of unique color.



Figure 8: Fond du Lac CIR Mosaic

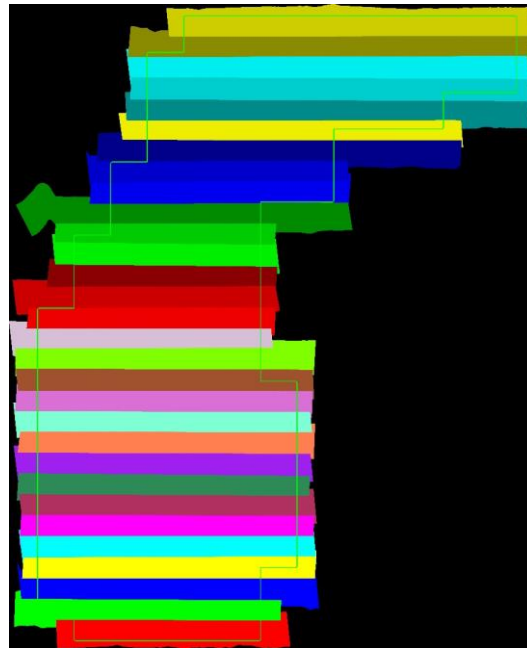


Figure 9: Fond du Lac LUT Mosaic

The flight line naming convention is derived from the date and time of collection, so a flight line listed as 0903-1500 was collected on 3 September at 3:00PM (15:00) local time. The following flight lines were used to compose the mosaic for the Fond du Lac site:

1. 0903-1455 (Northernmost Flight Line)
2. 0903-1500
3. 0903-1506
4. 0903-1512
5. 0903-1518
6. 0830-1219
7. 0830-1213
8. 0930-1209

9. 0830-1204
10. 0830-1200
11. 0830-1154
12. 0830-1150
13. 0830-1146
14. 0830-1142
15. 0830-1137
16. 0830-1132
17. 0830-1127
18. 0830-1122
19. 0830-1117
20. 0830-1113
21. 0830-1108
22. 0830-1103
23. 0830-1058
24. 0830-1053
25. 0830-1049
26. 0830-1044
27. 0830-1038
28. 0830-1033
29. 0830-1029
30. 0830-1023 (Southernmost Flight Line)

Site 2: St. Louis River Estuary

The St. Louis River Estuary site was collected over two days. On 1 September 2018, 18 lines were collected with four of them containing shadows and clouds. These four lines and the remaining 3 lines were collected on 3 September.

1. 0903-1544 (Northernmost Line)
2. 0903-1540
3. 0903-1535
4. 0901-1656
5. 0901-1651
6. 0901-1646
7. 0901-1641
8. 0901-1636
9. 0901-1631
10. 0901-1626
11. 0901-1621
12. 0901-1615
13. 0901-1607
14. 0901-1559
15. 0901-1543
16. 0901-1536
17. 0901-1532
18. 0903-1552
19. 0903-1557
20. 0903-1601 (Southernmost Line)

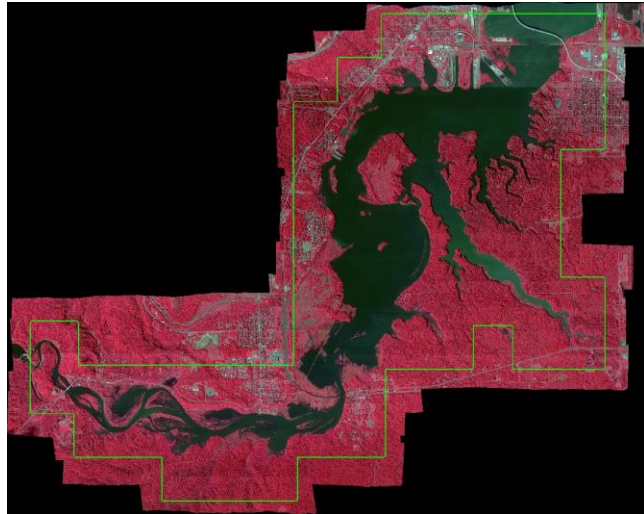


Figure 10: St. Louis River Estuary CIR Mosaic

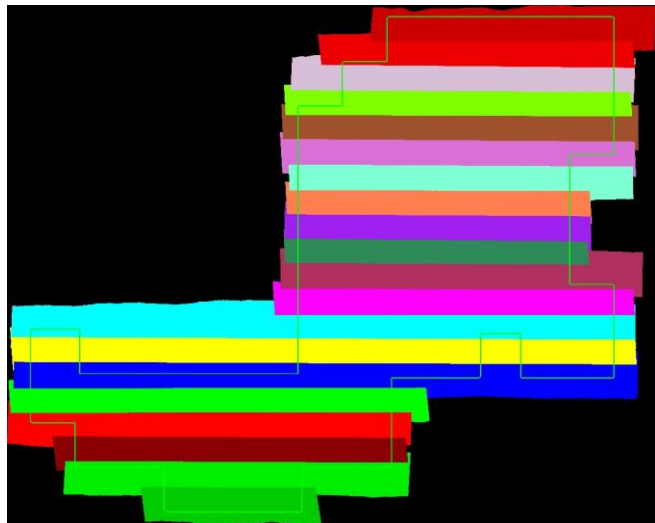


Figure 11: St. Louis River Estuary LUT Mosaic

Site 3: Upper St. Louis River

All 16 flight lines covering the Upper St. Louis River site were collected on 3 September 2018 under clear conditions with no re-collections necessary.

1. 0903-0943 (Northernmost)
2. 0903-0947
3. 0903-0950
4. 0903-0953
5. 0903-1002
6. 0903-1011
7. 0903-1019
8. 0903-1029
9. 0903-1037
10. 0903-1047
11. 0903-1056
12. 0903-1106
13. 0903-1115
14. 0903-1129
15. 0903-1133
16. 0903-1136 (Southernmost)

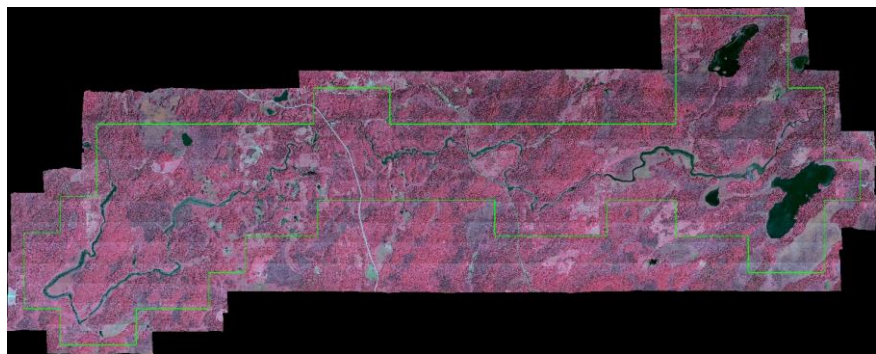


Figure 12: Upper St. Louis River CIR Mosaic

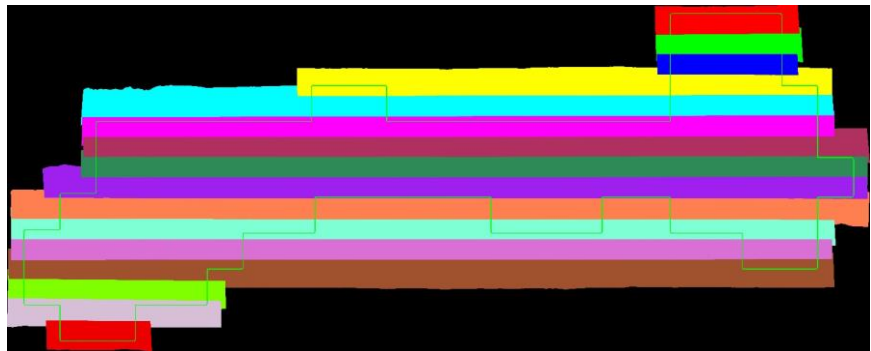


Figure 13: Upper St. Louis River LUT Mosaic

Site 4: Bad River and Kakagon Sloughs

All 15 flight lines covering the Bad River and Kakagon Sloughs site were collected on 6 Sept 2018 under clear conditions with no re-collections necessary.

1. 0906-0916 (Northernmost)
2. 0906-0921
3. 0906-0926
4. 0906-0931
5. 0906-0936
6. 0906-0941
7. 0906-0946
8. 0906-0952
9. 0906-1002
10. 0906-1009
11. 0906-1017
12. 0906-1024
13. 0906-1032
14. 0906-1040
15. 0906-1048 (Southernmost)

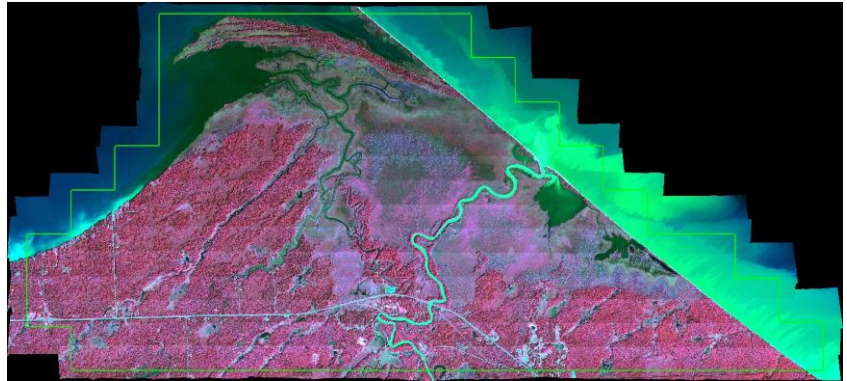


Figure 14: Bad River and Kakagon Sloughs CIR Mosaic

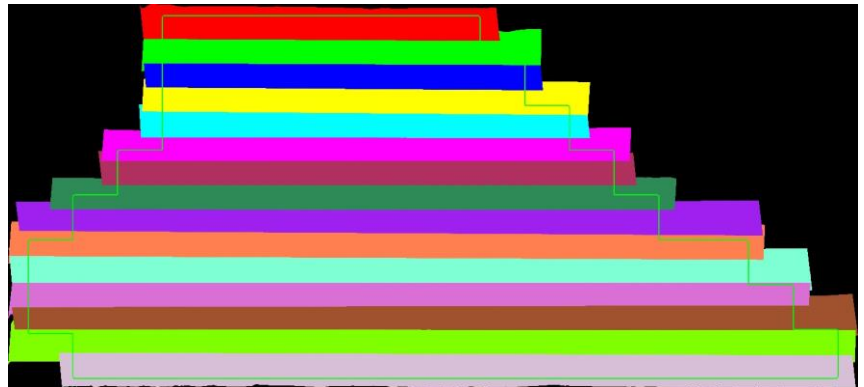


Figure 15: Bad River and Kakagon Sloughs LUT Mosaic

Site 5: Crooked Lake, Sucker Lake, and Ontonagon River

All 22 of the flight lines covering the Crooked Lake, Sucker Lake, and Ontonagon River site were collected on 6 September 2018 under clear conditions with no re-collections necessary.

1. 0906-1332 (Northernmost)
2. 0906-1324
3. 0906-1316
4. 0906-1307
5. 0906-1258
6. 0906-1249
7. 0906-1241
8. 0906-1233
9. 0906-1225
10. 0906-1217
11. 0906-1211
12. 0906-1206
13. 0906-1202
14. 0906-1159
15. 0906-1155
16. 0906-1151
17. 0906-1147
18. 0906-1144
19. 0906-1140
20. 0906-1137
21. 0906-1134
22. 0906-1131 (Southernmost)



Figure 16: Crooked Lake, Sucker Lake, and Ontonagon River CIR Mosaic

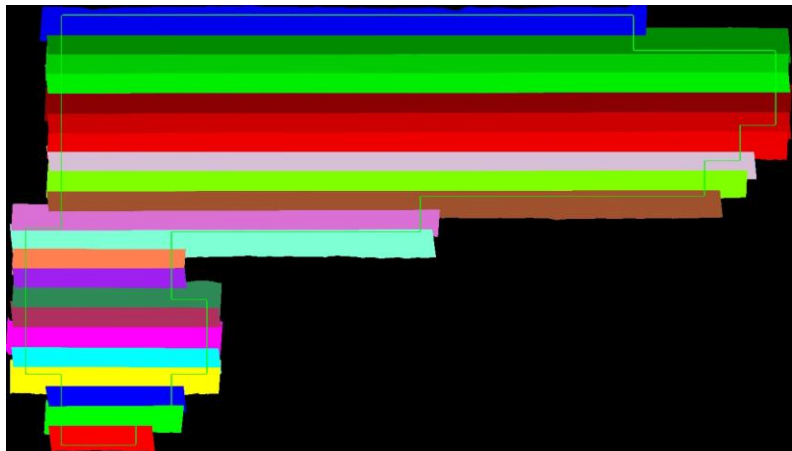


Figure 17: Crooked Lake, Sucker Lake, and Ontonagon River LUT Mosaic

Site 6: Eastern Upper Peninsula

All 13 of the flight lines covering the Eastern Upper Peninsula Site were collected on 7 Sept 2018 under clear conditions with no re-collections necessary.

1. 0907-1603 (Westernmost)
2. 0907-1606
3. 0907-1610
4. 0907-1614
5. 0907-1619
6. 0907-1622
7. 0907-1626
8. 0907-1631
9. 0907-1635
10. 0907-1640
11. 0907-1644
12. 0907-1648
13. 0907-1652 (Easternmost)

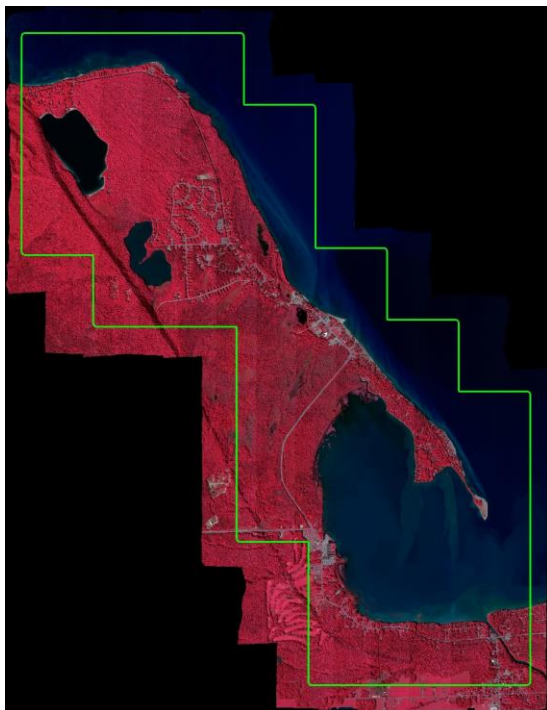


Figure 18: Eastern Upper Peninsula CIR Mosaic

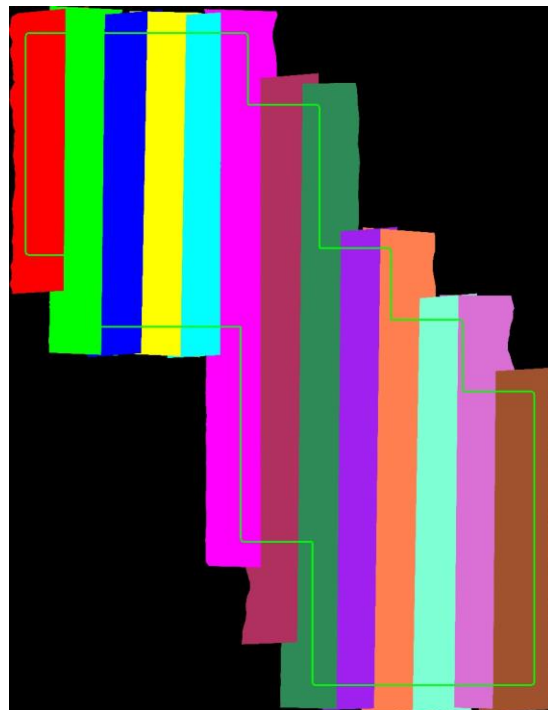


Figure 19: Eastern Upper Peninsula LUT Mosaic

Ground truthing data collection began on 6 September and last until 23 September. The Galileo Ground Truth crew consisted of Mr. Merrill and Galileo scientist, Gabriel Hoekstra. The crew visited each of the six AOI and collected GPS points, ground spectrometry and geo-tagged imagery. A canoe was the primary means of transport, but where this was not feasible, they took measurements from the shoreline or other access points. Please note that some of the spectrometer data was not included in the data delivery. This is because the spectrometer was sometimes triggered to collect when the crew was handling it to store it in a Pelican case onboard the canoe. These readings are essentially just noise and were therefore deemed unnecessary for delivery. Below are brief summaries and maps showing True Color (Red, Green, Blue) mosaics of the hyperspectral imagery overlaid by the ground truth data taken at each of the six AOI.

Site 1: Fond du Lac

Ground truthing operations at the Fond du Lac site started on 11 September 2018 when Mr. Merrill collected data for atmospheric correction at two different sites within the AOI. Extensive canoe expeditions on 16 September covered Perch Lake, Bang Lake and Rice Portage Lake. Big Lake, Twin Lakes and several inland sites near canals were visited and shoreline data was collected. In total, 228 geo-tagged images, 32 GPS points and 33 spectrometer readings were collected. Abundant Wild Rice mixed with Pickerelweed and Waterlily was found in Perch Lake, Bang Lake and Rice Portage Lake. However, no arrowhead was located and only sparse Phragmites was found throughout the AOI.



Figure 20: Perch Lake Wild Rice Geo-Tagged Image

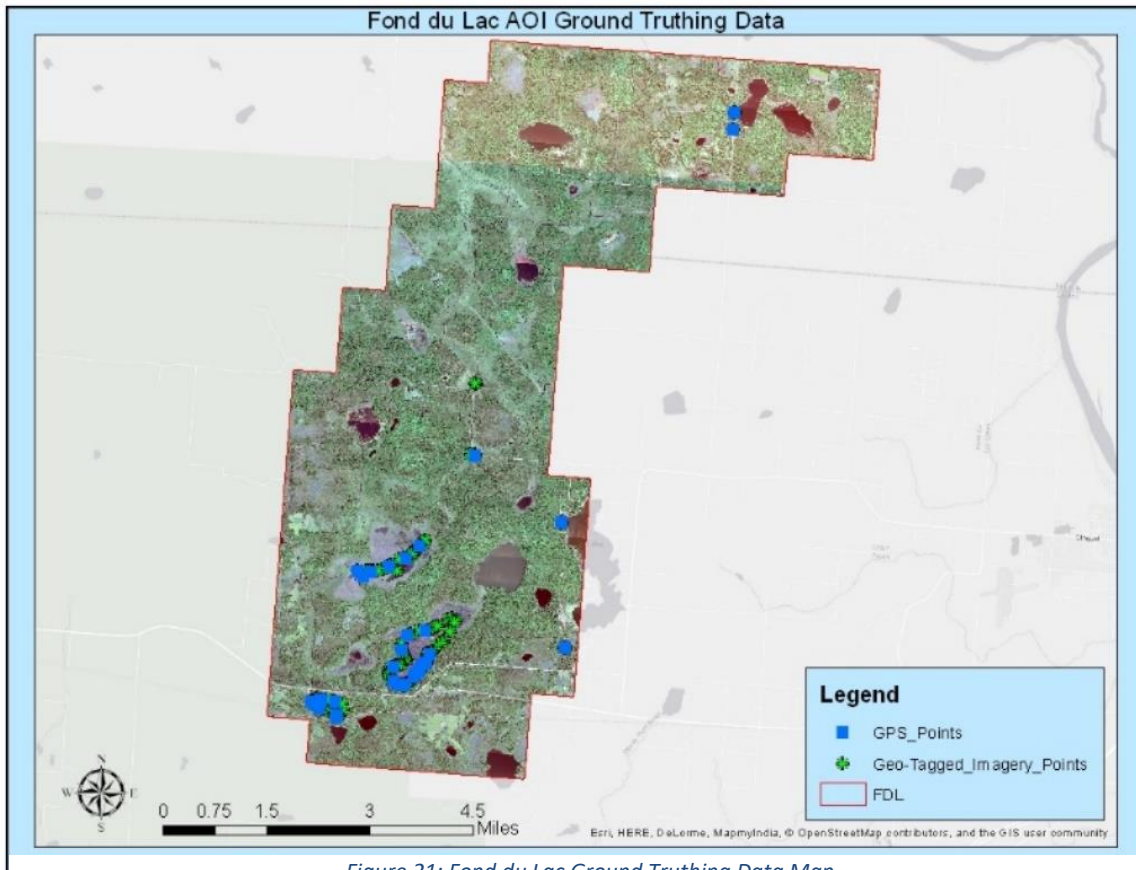


Figure 21: Fond du Lac Ground Truthing Data Map

Site 2: St. Louis River Estuary

Mr. Merrill began ground truthing operations on 11 September when he collected data at three locations for atmospheric correction. Then, three canoe expeditions were undertaken to cover the SLRE AOI on 13, 18, and 19 September. In total, 451 geo-tagged images, 62 GPS points and 15 spectrometer readings were collected. Only very sparse Wild Rice was located in SLRE and no Arrowhead, Phragmites, Pickerelweed or Watershield was found during ground truthing operations. However, large patches of Pondweed, Bulrush, Algae, Submersed Aquatic Vegetation (SAV) and Creeping Water Primrose were found.



Figure 22: Aquatic Vegetation in SLRE

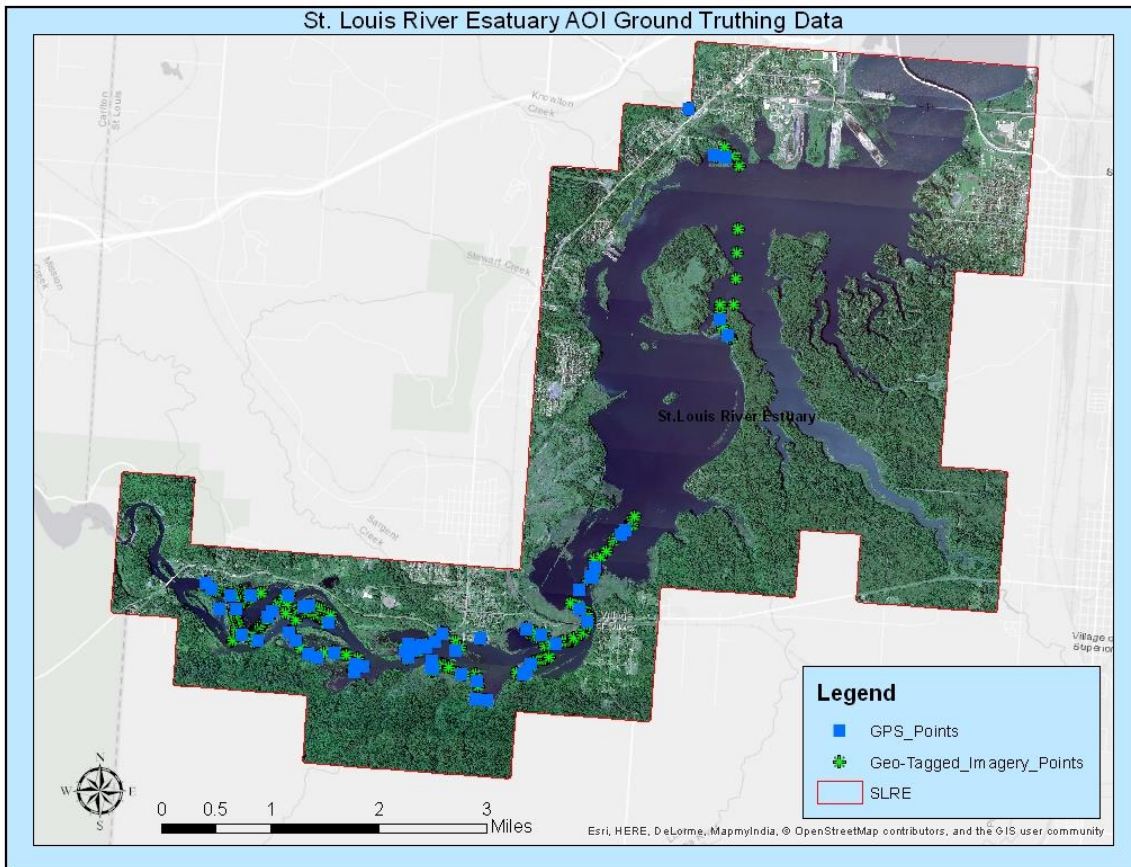


Figure 23: Saint Louis River Estuary Ground Truthing Data Map

Site 3: Upper St. Louis River

Atmospheric correction data collected on 11 September 2019 kicked off ground truthing operations in the Upper St. Louis River AOI. A very difficult canoe expedition was completed on 19 September. Low water conditions in areas of rocky rapids and several beaver dams forced the crew to hand carry the canoe filled with equipment for long stretches of the river. This slowed progress and forced the crew to abandon spectrometer and GPS points about ¾ of the way through the expedition due to low light. Abundant Wild Rice was found throughout the river, but no examples of Arrowhead, Phragmites or Watershield were located within the AOI. In total, 354 geo-tagged images, 14 GPS points and 27 spectrometer readings were collected here.



Figure 24: Beaver Dam on the Upper St. Louis River



Figure 25: Wild Rice and Pickerelweed on the Upper St. Louis River

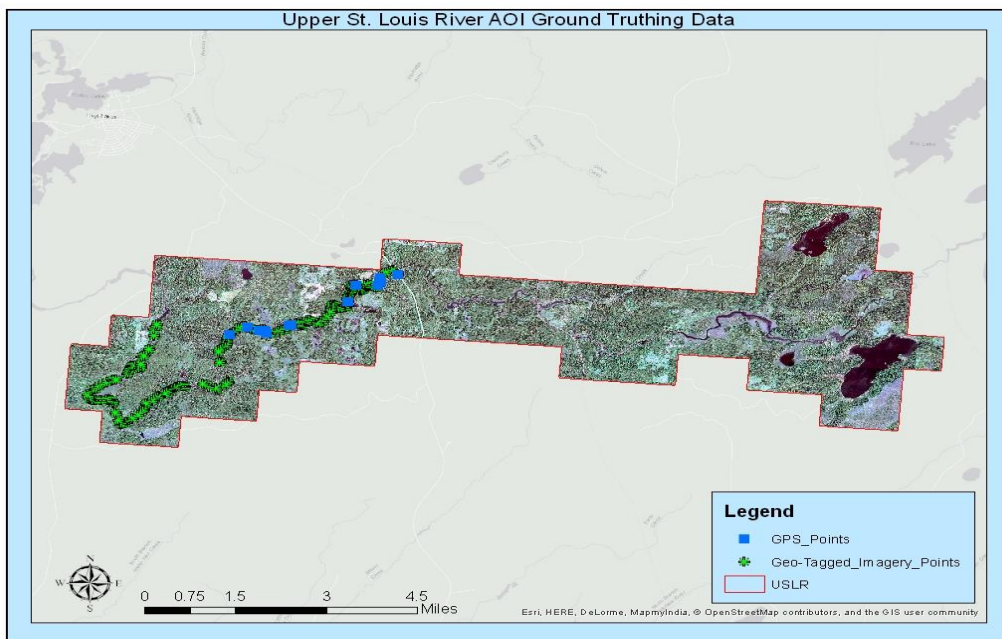


Figure 26: Upper St. Louis River Ground Truthing Data Map

Site 4: Kakagon Sloughs and Bad River

Jessica Strand, representing the Bad River Band of Lake Superior Chippewa, coordinated a motorboat for ground truthing operations on 13 September 2018. The crew was transported around the Kakagon Sloughs portion of the AOI where abundant Wild Rice was found throughout. However, no instances of Arrowhead, Phragmites, or Watershield were located. In total, 302 geo-tagged images, 35 GPS points and 36 spectrometer readings were collected in the Kakagon Sloughs and Bad River AOI.



Figure 27: Wild Rice in Kakagon Sloughs and Bad River

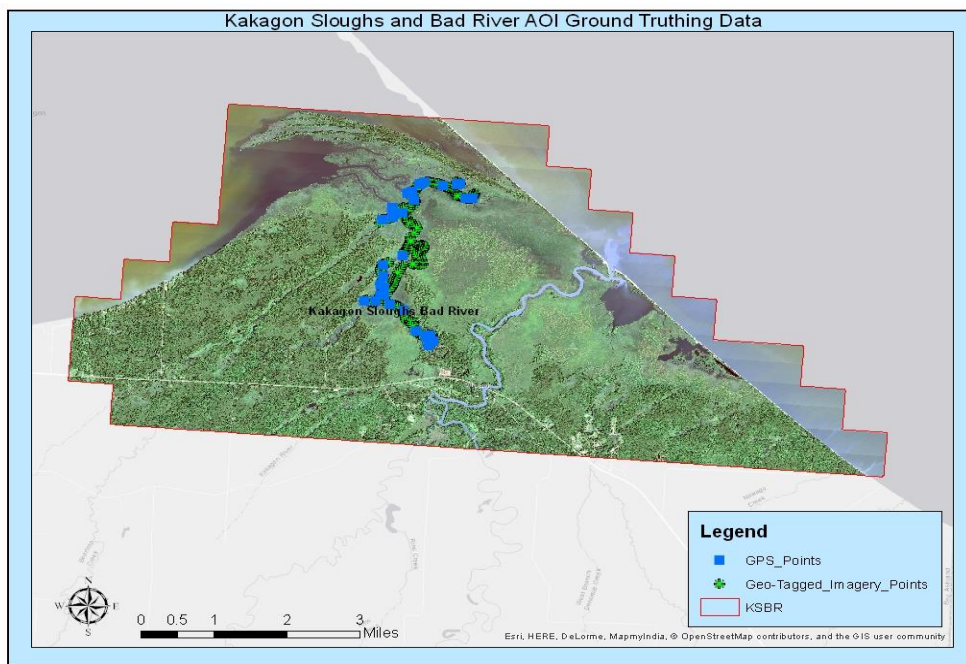


Figure 28: Kakagon Sloughs and Bad River Ground Truth Data Map

Site 5: Crooked Lake, Sucker Lake, and Ontonagon River

Ground truthing operations spanned two days at the Crooked Lake, Sucker Lake, and Ontonagon River Site. On 21 September 2018, the crew transited to the AOI by car and collected data along the shorelines of Sucker Lake, Bass Lake, Crooked Lake and Henderson Creek. The next day, a canoe expedition was completed along the Ontonagon River where large stands of Wild Rice were located starting near Sherman Pond and ending near the fork with the Tamarack River. In total, 192 geo-tagged images, 11 GPS points and 31 spectrometer readings were collected in the Crooked Lake, Sucker Lake and Ontonagon River AOI.



Figure 29: Wild Rice in the Ontonagon River

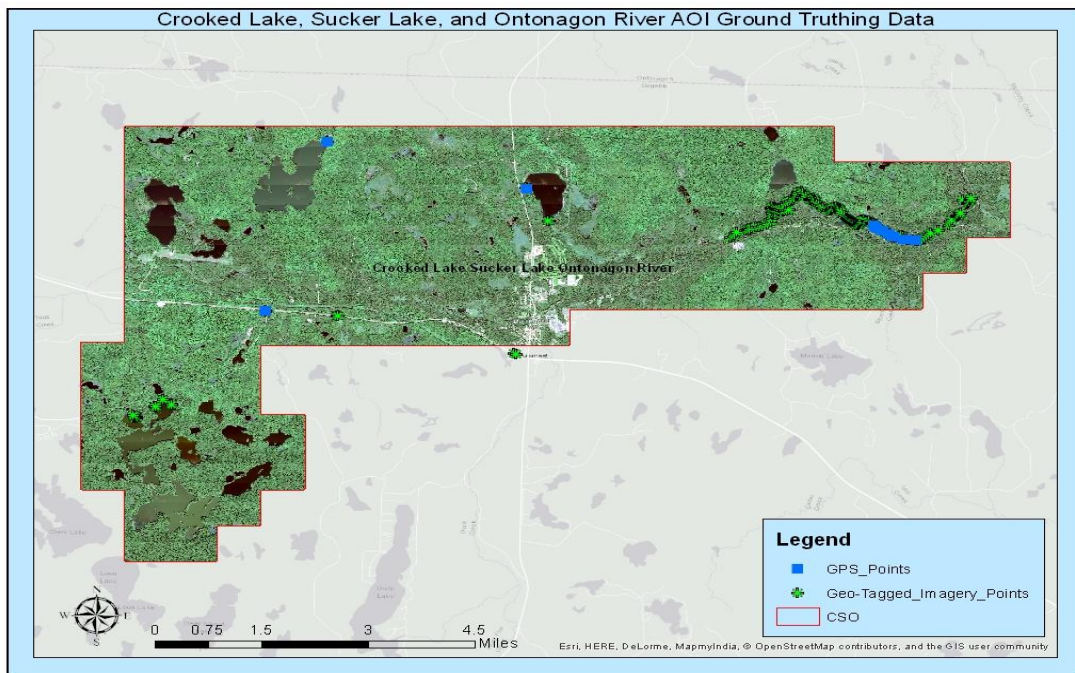


Figure 30: Crooked Lake, Sucker Lake and Ontonagon River Ground Truthing Data Map

Site 6: Eastern Upper Peninsula

On September 22 the crew transited to the Eastern Upper Peninsula and collected ground data for atmospheric correction. The next day, the crew completed a canoe expedition which covered the western halves of Waiska Bay and Back Bay. Small patches of Wild Rice were located during ground truthing at Spectacle Lake, but only small sparse patches. However, within Back Bay, large stands of bulrush, pondweed, Watershield and waterlily flourished with cattail and burred fringing the shore. Shoreline expeditions were also undertaken to cover wetlands around South Pond, North Pond and the southern extents of Spectacle Lake and Monocle Lake. Please note the strong winds and rough waves forced the crew to abandon spectrometer and GPS collection in this area. In total, 190 geo-tagged images, 1 GPS point, and 18 spectrometer readings were collected in the Eastern Upper Peninsula AOI.



Figure 31: Watershield in Back Bay

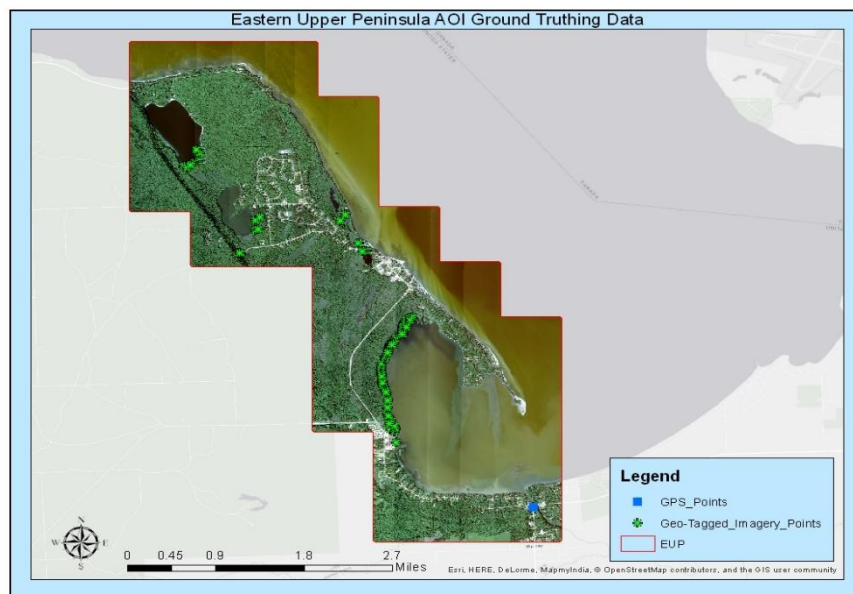


Figure 32: Eastern Upper Peninsula Ground Truthing Data Map

4. Data Processing and QC

As soon as the aircraft returned to base, Mr. Merrill made a copy of the raw data collected that day and began data processing on his field laptops using ENVI software and Galileo's proprietary Project Manager software. The following section details the steps taken to pre-process the data.

Processing Level 1a – Radiometric Correction

1. Dark Noise Removal

Dark image data was acquired for every raw image at the end of every flight line by the sensor control software closing the shutter and recording 5 seconds of dark noise. To remove sensor noise the mean value of every line of the dark data was subtracted from the corresponding line of the raw data (dark noise removal or dark current removal).

2. Calibration from RAW data to radiance data using calibration file

After the dark noise removal, the raw data was calibrated to radiance units using a sensor specific calibration file. Every spatial and spectral pixel is multiplied with the corresponding value in the calibration file. The calibration values for each pixel on the CCD are calculated using an integrating sphere in the laboratory.

The radiance units are equal to $(\text{mW}/\text{cm}^2 \cdot \text{str} \cdot \mu\text{m}) \cdot 1000.00$.

3. Smile Correction

Spectral smile is defined as changes in wavelength over the field of view (FOV). Smile correction was performed by proprietary algorithms.

4. Crosstrack Correction

A crosstrack correction was performed using proprietary algorithm in order to normalize illumination in the across-track direction of each flight line.

5. Quality Control

Quality control was accomplished using ASD measurements, established radiometric quality protocols and systematic manual evaluations.

Processing Level 1b – Atmospheric Correction

1. Atmospheric Correction

The radiance units were converted to reflectance units using the ASD spectrometer measurements of uniform surfaces (parking lots, asphalt, sand and concrete) that were collected in the field. Multiple spectrometer measurements were taken at each site under clear conditions to ensure data quality. An “empirical line correction” method was used to calibrate every flight line to reflectance. After the correction an adaptive spectral filter was used to smooth the reflectance values and to eliminate outliers and spikes in the spectra.

The reflectance units are equal to Reflectance*10000.

2. Quality Control

Quality control was accomplished using ASD spectrometer measurements, established atmospheric correction quality protocols and systematic manual evaluations.

Processing Level 2 – Geometric Correction

1. Calculation of the sensor offset (Boresight correction)

During the aerial acquisition, four special Boresight flight lines were flown to geometrically calibrate the sensor and GPS/INS. The Boresight parameters were calculated using four overlapping flight lines flown in a crosshair pattern. 15 to 20 Ground Control Points per flight line pair (GCPs) were identified and used to calculate geometric correction values for Roll (0.162353), Pitch (0.131388) and Yaw (0.166983). These values were then used as input parameters for the geometric correction process.

2. GPS/INS Data

The GPS/INS Data was encoded and processed for the use in the georectification process

3. GLT files (Geographic Lookup Table)

A GLT file contains the geographic location of every pixel in the unrectified reflectance data. A GLT file was generated for every flight line using the GPS/INS Data, the Boresight Correction parameters and a Digital Elevation Model (DEM)

Processing Level 3 – Orthorectification

1. Georectification using GLT data

The unrectified reflectance data was then Georectified into North American Datum of 1983 (NAD83) and projected into the Universal Transverse Mercator (UTM) coordinate system using the corresponding GLT file. A DEM was used to correct for surface elevation variation across the scene.

2. Mosaicking

Individual flight lines for each AOI were combined into a single mosaic image which covered the entire AOI. This image was then masked to the AOI boundary and tiled according to the tiling scheme vectors included with this delivery.

3. Quality Control

Geo-accuracy was checked and confirmed to meet pre-established quality standards by systematic comparison of specific geo-locations acquired in the field with a GPS unit and high resolution RGB imagery of known geo-accuracy.

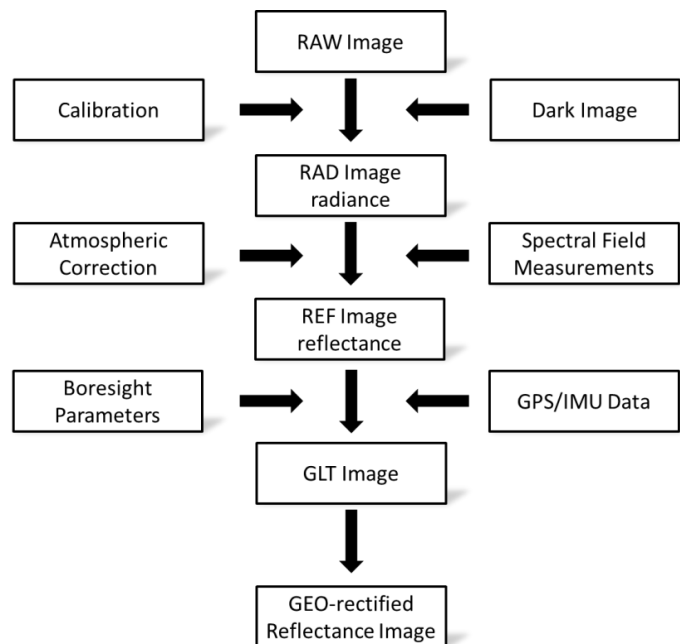


Figure 33: Hyperspectral Pre-Processing Workflow

5. Analysis

At the conclusion of data pre-processing, Mr. Merrill utilized the ortho-rectified 128 band reflectance mosaics of each AOI as the inputs for spectral analysis. In order to eliminate areas such as roads/urban, upland forests and other non-wetlands areas, masks were then created for the shoreline and islands within the study area. This helped reduce false positives and processing time. These masks were then applied to the full band mosaics and the resulting masked images were used as the final imagery input data for classification. Below is an image showing the resulting masked mosaic on the right and the input unmasked mosaic on the left.

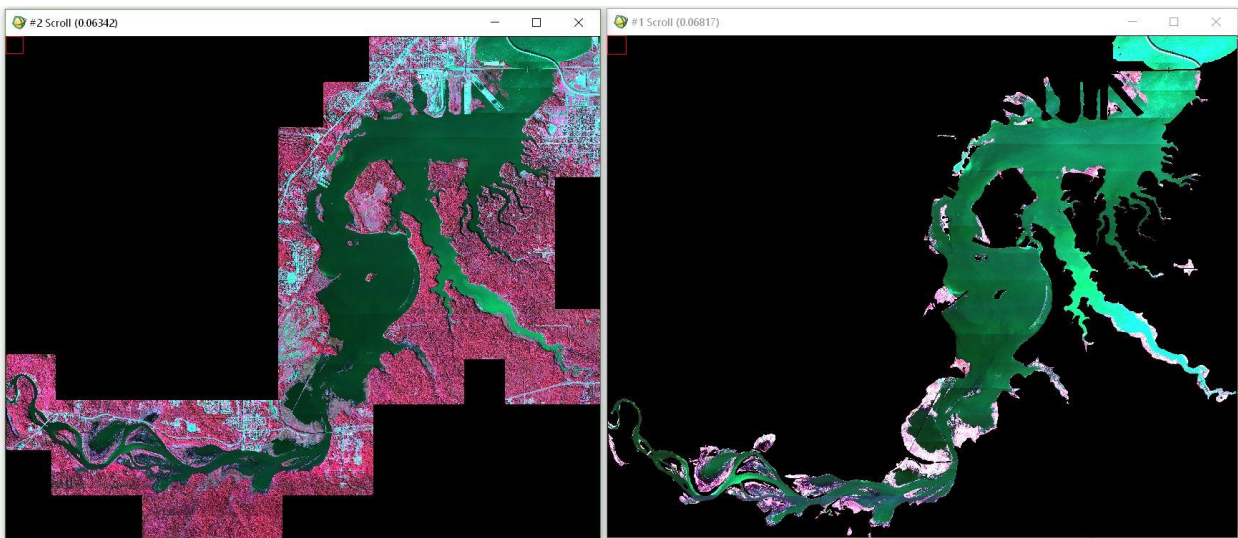


Figure 34: SLRE Analysis Masking Example

The ground truthing data was then overlaid on these mosaics in order to identify known locations of target vegetation. Using these known locations, Mr. Merrill then created Regions of Interest (ROI) to isolate pixels of individual species and extract their spectral signatures from the full band mosaic and into a spectral library. The ground spectrometry data was also used as an input for the Wild Rice spectral library, but all other classes were created from this in-scene spectral extraction method. Several non-target species were also captured in this way in order to separate them into the Other Emergent Aquatic Vegetation class. These species include, pondweed, bulrush, grasses, black willow and others.

Please note that in order to capture the variability inherent within each species and class, multiple ROI inputs were used to create each spectral library. For example, Wild Rice was seen to be green and healthy in Bang Lake, but yellow to brown in Perch Lake, so multiple spectra were extracted from these different

locations to create the spectral library and thereby capture the variability of the species. This approach was common for all classes.

Next, the spectral libraries were carefully examined, and outlying pixels were eliminated in order to create a more cohesive and uniform signature for each resulting endmember. These endmembers were then used as inputs for a proprietary Supervised Classification algorithm which utilized the Spectral Angle Mapper (SAM) method found in ENVI software as well as other proprietary methods and steps. Upon the completion of Supervised Classification, a class image containing one class per endmember was created. Mr. Merrill then carefully reviewed the results, refined the endmembers and classification parameters and re-ran the classification algorithm until a classification image representative to the conditions observed on the ground was achieved. Endmember classes of the same species/class were then combined into a single class and several post-classification algorithms were run to eliminate outlying pixels and consolidate classes. The final classified vectors were then converted to vector polygons and manually inspected to ensure accuracy and the highest data quality.

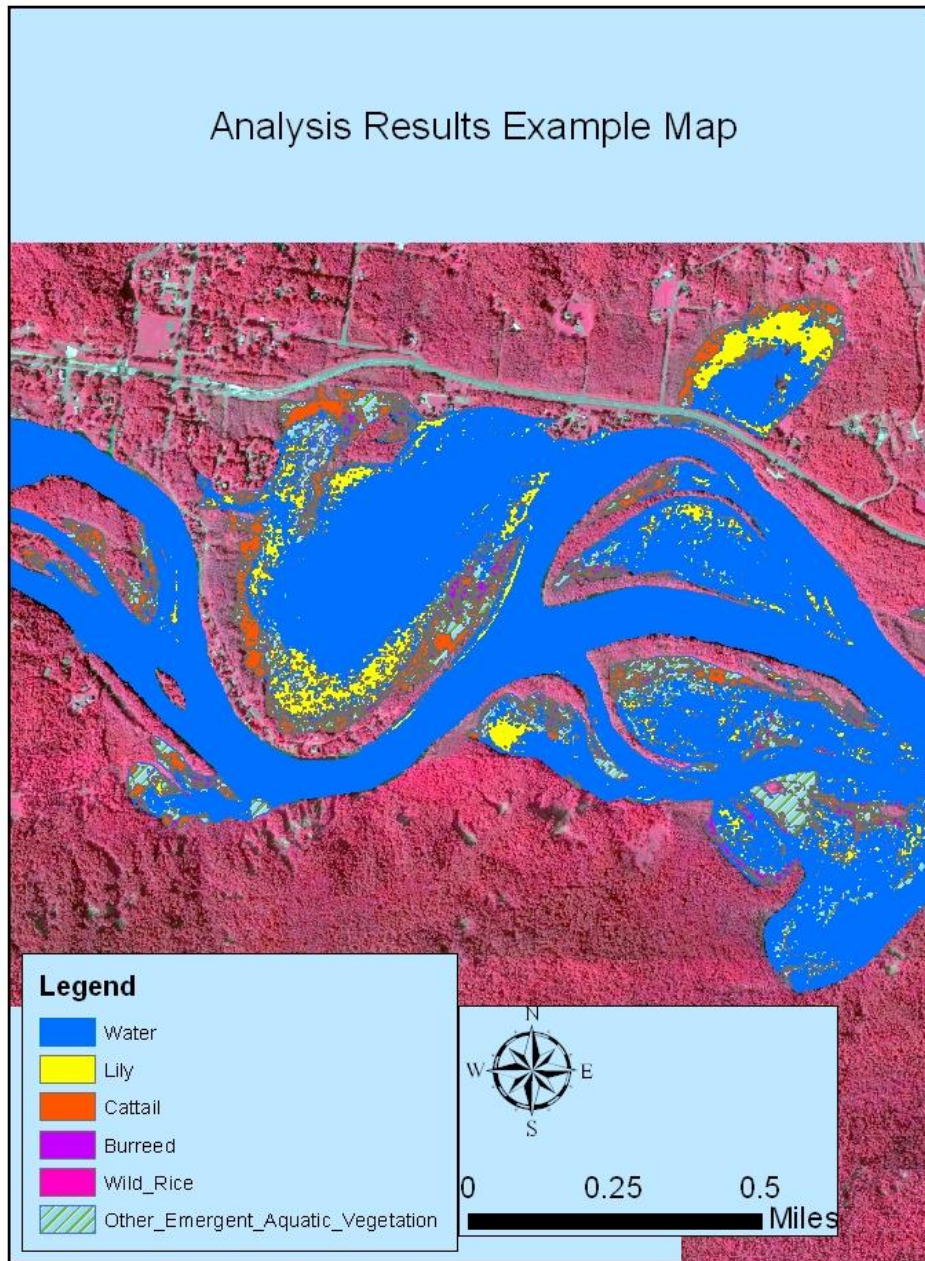


Figure 35: Analysis Results Example Map

6. Conclusion

Large stands of Wild Rice in the CSO, FDL, KSBR, and USLR allowed for highly accurate delineation when compared to known ground data of this species of primary concern. It was also helpful that the species which were commonly found to mix with Wild Rice, namely Pickerelweed, Waterlily, Burreed, Cattail, and Bulrush were still mainly green and photosynthesizing, while the majority of Wild Rice had begun senescence. Although, green Wild Rice in the CSO and small patches in KSBR still showed strong spectral separation from other nearby green vegetation plant structure, chlorophyll content, spatial pattern, and density of the stands varied greatly from the previously listed commonly mixed species.

In order to provide additional quantitative insight into the analysis results, I have also created a spreadsheet detailing the acreage of each class in each AOI and their percentage of total vegetation classified. Please note that the Open Water class is left out of this vegetation calculation. This spreadsheet is titled NIGHTHAWK Species Acreage.xlsx and can be found in the documents folder for this delivery. Additional informatics are available upon request.

Galileo Group appreciates the opportunity to be of service to you and your team. Please feel free to contact us anytime if there are any questions regarding the data and the deliverables. We would be happy to assist you.

Sincerely,



John Merrill

Operations Officer

615.427.8871

jmerrill@galileo-gp.com

Appendix A

Galileo Flight Log									
Project	Date	Operator	Solar Window	GSD	Desired Altitude	Weather		Total Engine Runtime	Aircraft Tail #\Aircraft Type\Vendor
NIGHTHAWK	20180830	JM		1.0m	5850	Clear to scattered			N1419D, Chapa
Spectral Binning	4	Speed	100						
Spacial Binning	1	Frame Rate	56						
Line#	APR All/Partial/Reflight	Heading	Altitude	Speed	Integration Time	Frame Rate	Lost Frames	Dark Image	Comments
1023		W	5850	100	14	56		Auto	Southernmost Line of Fond du Lac Site
1029		E	5850	100	14	56		Auto	
1033		W	5850	100	14	56		Auto	
1038		E	5850	100	14	56		Auto	
1044		W	5850	100	14	56		Auto	
1049		E	5850	100	14	56		Auto	
1053		W	5850	100	14	56		Auto	
1058		E	5850	100	14	56		Auto	
1103		W	5850	100	14	56		Auto	
1108		E	5850	100	14	56		Auto	
1113		W	5850	100	14	56		Auto	
1117		E	5850	100	14	56		Auto	
1122		W	5850	100	12	56		Auto	
1127		E	5850	100	12	56		Auto	
1132		W	5850	100	12	56		Auto	
1142		E	5850	100	12	56		Auto	
1146		W	5850	100	12	56		Auto	
1150		E	5850	100	12	56		Auto	
1154		W	5850	100	12	56		Auto	
1200		E	5850	100	12	56		Auto	
1204		W	5850	100	12	56		Auto	
1209		E	5850	100	12	56		Auto	
1213		W	5850	100	12	56		Auto	
1219		E	5850	100	12	56		Auto	
1224		W	5850	100	12	56		Auto	Shadows, bad data, refly
1229		E	5850	100	12	56		Auto	Shadows and clouds, bad data, refly
1235		W	5850	100	12	56		Auto	Shadows and clouds, bad data, refly
1240		E	5850	100	12	56		Auto	Shadows and clouds, bad data, refly
1246		W	5850	100	12	56		Auto	Northernmost line Shadows and clouds, bad data, refly
1301		E	4100	100	5	75		Auto	Boresight
1305		W	4100	100	5	75		Auto	Boresight
1310		S	4100	100	5	75		Auto	Boresight
1313		N	4100	100	5	75		Auto	Boresight

Figure 36: 30 Aug 2018 Flight Log

Galileo Flight Log									
Project	Date	Operator	Solar Window	GSD	Desired Altitude	Weather		Total Engine Runtime	Aircraft Tail #\Aircraft Type\Vendor
NIGHTHAWK	9/1/2018	JM		1.0m	5300	Scattered to clear			N1419D, Chapa
Spectral Binning	4	Speed	100						
Spacial Binning	1	Frame Rate	56						
Line#	APR All/Partial/Re flight	Heading	Altitude	Speed	Integration Time	Frame Rate	Lost Frames	Dark Image	Comments
1045		N	5300	100	12	56		Auto	Easternmost, St. Louis River Site, Clouds, bad data
1517		W	5300	100	12	56		Auto	Southernmost St. Louis River Estuary Site, shadow SW corner, bad data, refly
1521		E	5300	110	12	62		Auto	Shadows SW corner, bad data, refly
1526		W	5300	100	12	56		Auto	Shadows SW corner, bad data refly
1532		E	5300	110	12	62		Auto	
1536		W	5300	100	12	56		Auto	
1543		E	5300	110	12	62		Auto	
1559		W	5300	90	12	50		Auto	
1607		E	5300	110	12	62		Auto	
1615		W	5300	90	12	50		Auto	
1621		E	5300	110	12	62		Auto	
1626		W	5300	90	12	50		Auto	
1631		E	5300	110	12	62		Auto	
1636		W	5300	90	12	50		Auto	
1641		E	5300	110	12	62		Auto	
1646		W	5300	90	12	50		Auto	
1651		E	5300	110	12	62		Auto	
1656		W	5300	90	12	50		Auto	

Figure 37: 1 September 2018 Flight Log

Galileo Flight Log									
Project	Date	Operator	Solar Window	GSD	Desired Altitude	Weather		Total Engine Runtime	Aircraft Tail #\Aircraft Type\Vendor
NIGHTHAWK	3-Sep	JM		1.0m		Clear			N1419D, Chapa
Spectral Binning	4	Speed	100						
Spacial Binning	1	Frame Rate	56						
Line#	APR All/Partial/Reflight	Heading	Altitude	Speed	Integration Time	Frame Rate	Lost Frames	Dark Image	Comments
943		E	6200	100	12	56		AUTO	Upper St. Louis River Site, Northernmost line
947		W	6200	100	12	56		AUTO	
950		E	6200	100	12	56		AUTO	
953		W	6200	100	12	56		AUTO	
1002		E	6200	100	12	56		AUTO	
1011		W	6200	100	12	56		AUTO	
1019		E	6200	100	12	56		AUTO	
1029		W	6200	100	12	56		AUTO	
1037		E	6200	100	12	56		AUTO	
1047		W	6200	100	12	56		AUTO	
1056		E	6200	100	12	56		AUTO	
1106		W	6200	100	12	56		AUTO	
1115		E	6200	100	12	56		AUTO	
1129		W	6200	100	12	56		AUTO	
1133		E	6200	100	12	56		AUTO	
1136		W	6200	100	12	56		AUTO	Upper St. Louis River Site, Southernmost line
1200	Reflight	E	5900	100	12	56		AUTO	Fond du Lac Northernmost, Clouds and shadows Bad data
1206	Reflight	W	5900	100	12	56		AUTO	Clouds and shadows, bad data
1455	Reflight	W	5900	100	14	56		AUTO	Fond du Lac Northernmost line, good data
1500	Reflight	E	5900	100	14	56		AUTO	
1506	Reflight	W	5900	100	14	56		AUTO	
1512	Reflight	E	5900	100	14	56		AUTO	
1518	Reflight	W	5900	100	14	56		AUTO	
1535		E	5300	100	14	56		AUTO	St. Louis River Estuary Site 3rd from N
1540		W	5300	100	14	56		AUTO	
1544		E	5300	100	14	56		AUTO	St. Louis River Estuary Site, Northernmost
1552	Reflight	W	5300	100	14	56		AUTO	St. Louis River Estuary Site 3rd from S
1557	Reflight	E	5300	100	14	56		AUTO	
1601	Reflight	W	5300	100	14	56		AUTO	St. Louis River Estuary Site Southernmost

Figure 38: 3 September 2018 Flight Log

Galileo Flight Log									
Project	Date	Operator	Solar Window	GSD	Desired Altitude	Weather		Total Engine Runtime	Aircraft Tail #\Aircraft Type\Vendor
NIGHTHAWK	9/6/2018	JM		1.0m		Clear			N1419D, Chapa
Spectral Binning	4	Speed	100						
Spacial Binning	1	Frame Rate	56						
Line#	APR AIMP Partial Reflight	Heading	Altitude	Speed	Integration Time	Frame Rate	Lost Frames	Dark Image	Comments
916		E	5100	100	12	56		Auto	Bad River Site, Northernmost line
921		W	5100	100	12	56			
926		E	5100	100	12	56			
931		W	5100	100	12	56			
936		E	5100	100	12	56			
941		W	5100	100	12	56			
946		E	5100	100	12	56			
952		W	5100	100	12	56			
1002		E	5100	100	12	56			
1009		W	5100	100	12	56			
1017		E	5100	100	12	56			
1024		W	5100	100	12	56			
1032		E	5100	100	12	56			
1040		W	5100	100	12	56			
1048		E	5100	100	12	56			Bad River Site, Southernmost line
1056		W	5100	100	12	56			Refight, Not needed
1131		E	6300	100	12	56			Ontonagon Site, Southernmost Line
1134		W	6300	100	12	56			
1137		E	6300	100	12	56			
1140		W	6300	100	12	56			
1144		E	6300	100	12	56			
1147		W	6300	100	12	56			
1151		E	6300	100	12	56			
1155		W	6300	100	12	56			
1159		E	6300	100	12	56			
1202		W	6300	100	12	56			
1206		E	6300	100	12	56			
1211		W	6300	100	12	56			
1217		E	6300	100	12	56			
1225		W	6300	100	12	56			
1233		E	6300	100	12	56			
1241		W	6300	100	12	56			
1249		E	6300	100	12	56			
1258		W	6300	100	12	56			
1307		E	6300	100	12	56			
1316		W	6300	100	12	56			
1324		E	6300	100	12	56			
1332		W	6300	100	12	56			Ontonagon Site, Northernmost line

Figure 39:6 September 2018 Flight Log

Galileo Flight Log									
Project	Date	Operator	Solar Window	GSD	Desired Altitude	Weather		Total Engine Runtime	Aircraft Tail #\Aircraft Type\Vendor
NIGHTHAWK	9/7/2018	JM		1.0m	5300	Clear			N1419D, Chapa
Spectral Binning	4	Speed	100						
Spacial Binning	1	Frame Rate	56						
Line#	APR All/Partial/Re flight	Heading	Altitude	Speed	Integration Time	Frame Rate	Lost Frames	Dark Image	Comments
1603		N	5300	90	12	50		Auto	Eastern Upper Peninsula Site, Westernmost Line
1606		S	5300	120	12	62		Auto	
1610		N	5300	90	12	50		Auto	
1614		S	5300	120	12	62		Auto	
1619		N	5300	90	12	50		Auto	
1622		S	5300	120	12	62		Auto	
1626		N	5300	90	12	50		Auto	
1631		S	5300	120	12	62		Auto	
1635		N	5300	90	12	50		Auto	
1640		S	5300	120	12	62		Auto	
1644		N	5300	90	12	50		Auto	
1648		S	5300	120	12	62		Auto	
1652		N	5300	90	12	50		Auto	Eastern Upper Peninsula Site, Easternmost Line

Figure 40:7 September 2018 Flight Log

Appendix B

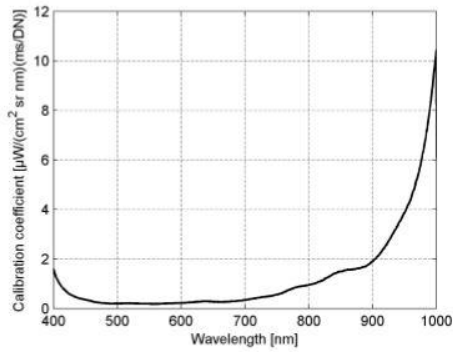


Figure Radiometric 1.
Radiometric calibration coefficient.

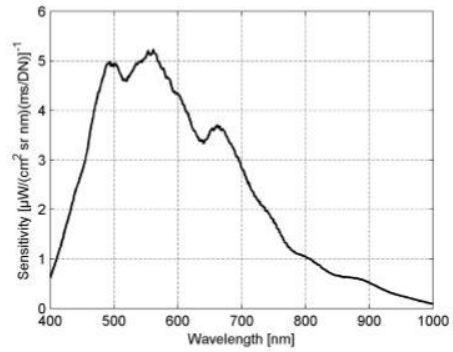


Figure Radiometric 2.
Radiance sensitivity of the sensor.

Figure 41: AISA Eagle II Sensor Radiometric Calibration Coefficient and Radiance Sensitivity

END